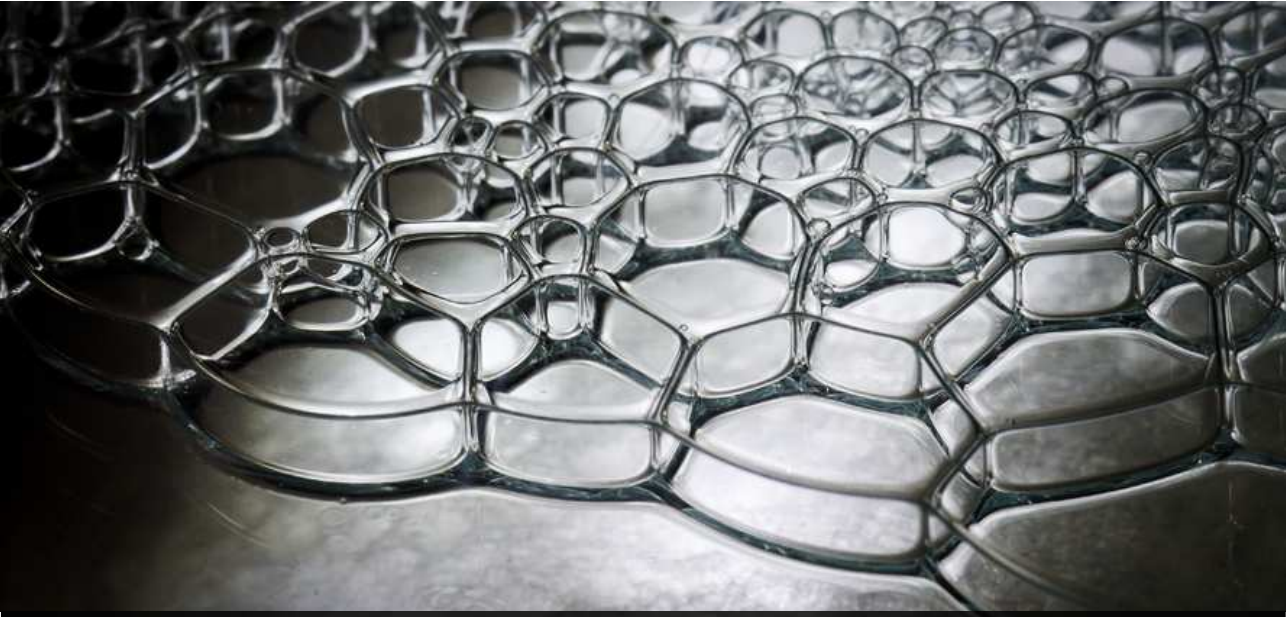


Chapter 8

Nonlinear Plane Waves in Frequency Power Law Attenuation Media

Abstract

In this chapter we revise fundamental aspects of nonlinear acoustic plane wave propagation through frequency power law attenuation media, with special focusing in the implications for finite amplitude ultrasound in biological media. The basic relationships between nonlinearity, absorption and dispersion are explored in detail, among with its implications for soft-tissue modeling in biomedical ultrasound applications. A derivation of simple expressions for quantify the role of the exponent of the power law in the balance between nonlinearity, dispersion and attenuation is presented. Detailed numerical calculations of the harmonic generation are also provided, where the efficiency in the harmonic generation and its relation with the weak frequency power law dispersion is studied.

8.1 Introduction

When modeling longitudinal acoustic wave propagation in biological soft-tissue media it is critical to account for the correct attenuation and phase speed. When dealing with linear monochromatic propagation, the values of media attenuation and phase speed for a given frequency can be explicitly included in the model equations from those obtained from experimental tests. A common practice is to adopt a sound speed value from the experimentally measured phase speed as $c_0 = c_p(\omega_0)$, and to match a value for the fluid viscosity, μ, that match the attenuation value at the desired frequency. However, if finite amplitude propagation is considered, the attenuation and phase velocity of each spectral component must be explicitly included in the model. In the case of biological media, where frequency power law attenuation is experimentally observed, there it is impossible to model these losses with only viscosity as long viscous losses present a frequency squared dependent attenuation and no dispersion. Thus, the inclusion of a causal-time domain operator that models frequency power law attenuation is necessary to accurately model the losses of each spectral component. Moreover, the inclusion of a frequency power law leads to the inevitable inclusion of dispersion that must be accurately modeled. Thus, for a frequency dependent attenuation in the form

$$\alpha(\omega) = \alpha_0 \omega^{\gamma}, \tag{8.1}$$

and by applying the Kramers-Kronig relationships (O'Donnell et al., 1981), the frequency dependent phase speed can be obtained as (Waters et al., 2005):

$$\frac{1}{c_p\left(\omega\right)} = \frac{1}{c_0} + \alpha_0 \tan\left(\frac{\pi\gamma}{2}\right)\left(|\omega|^{\gamma-1} - |\omega_0|^{\gamma-1}\right). \tag{8.2}$$

This expression is valid in the range $0 < \gamma < 3$ with $\gamma \neq 1$ and includes causality. In the limit $\gamma \to 1$ Eq. 8.2 reduces to

$$\left.\frac{1}{c_p\left(\omega\right)}\right|_{\gamma=1} = \frac{1}{c_0} - \frac{2}{\pi}\alpha_0 \log\left|\frac{\omega}{\omega_0}\right|. \tag{8.3}$$

On the other hand, the complex wave number $\tilde{k}$ can be written as

$$\tilde{k}\left(\omega\right) = \frac{\omega}{c_p\left(\omega\right)} - i\alpha\left(\omega\right), \tag{8.4}$$

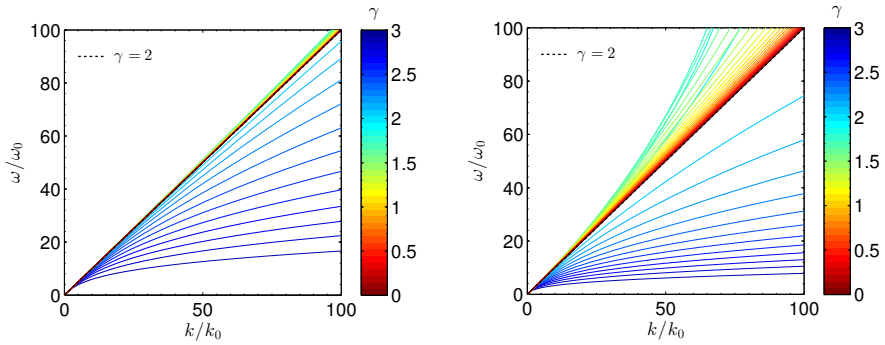


Figure 8.1: Dispersion relations for different frequency power laws for (a) $\alpha_0 = 10$ dB/cm and (b) $\alpha_0 = 1$ dB/cm measured at 1 MHz.

where $\mathrm{Im}(\tilde{k})$ is defined by the frequency power law attenuation and $\mathrm{Re}(\tilde{k})$ defines the phase speed. Combining Eq. 8.2, 8.1 and 8.4 the dispersion relations for a frequency power law media read

$$\tilde{k}\left(\omega\right) = \frac{\omega}{c_0} + \alpha_0 \omega \tan\left(\frac{\pi\gamma}{2}\right)\left(\left|\omega\right|^{\gamma-1} - \left|\omega_0\right|^{\gamma-1}\right) - i\alpha_0\omega^{\gamma} \tag{8.5}$$

for $0 < \gamma < 1$ and $1 < \gamma < 3$, and

$$\tilde{k}\left(\omega\right)\Big|_{\gamma=1} = \frac{\omega}{c_0} - \frac{2\alpha_0\omega}{\pi}\log\left|\frac{\omega}{\omega_0}\right| - i\alpha_0\omega \tag{8.6}$$

for $\gamma = 1$.

Thus, as shown in Fig. 8.1, the dispersion modeled by a frequency power law shows three different behavior depending on the power law exponent. First, for frequency independent losses, $\gamma = 0$, the media exhibit no dispersion as long $c_p = c_0$. This behavior is equivalent to the other simple physical attenuation models, e.g. the damped pendulum. On the other hand, this dispersionless regime is achieved also for $\gamma = 2$, as it is observed in acoustics for bulk thermo-viscous losses in pure water. Second, for $0 < \gamma < 2$ the real part of the wavenumber reduces in magnitude as long the frequency increases, so phase speed is increased in the higher frequency range, leading to the so called "anomalous dispersion" (Hill et al., 2004) (e.g. as observed also in water capillary waves). Finally, for media obeying frequency power law attenuation with $2 < \gamma < 3$ the phase speed decreases with increasing frequency, so "normal" dispersion is achieved as observed in other common physical systems as water surface gravity waves.

The frequency power law attenuation obtained for a soft-tissue media with an attenuation of 1 dB/cm and for 10 dB/cm measured at 1 MHz is shown in

Fig. 8.2. In the same way, Fig. 8.3 shows the frequency dependent phase speed from Eq. (8.2, 8.3), where for a frequency range from 0.1 to 10 MHz variations of about ±9 m/s are obtained in the case of 1 dB/cm at 1 MHz, and ≈ ±90 m/s for the case of 10 dB/cm for a linear power law. Thus, the magnitude of the dispersion of the system increases linearly with the attenuation magnitude. This behavior is in agreement with dispersion measurements in weakly (Szabo, 1995; Waters et al., 2000) and strongly (Fry et al., 1978) lossy media obeying frequency power law attenuation, and shows the importance of modeling correctly not only the attenuation but the dispersion when dealing with high damped media as biological tissues.

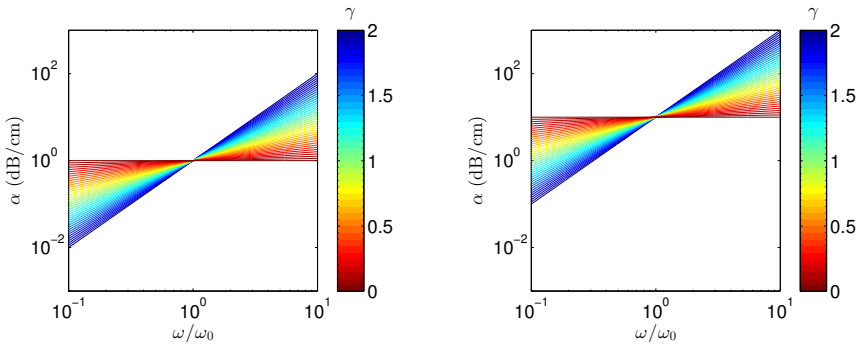


Figure 8.2: Frequency dependent attenuation obtained for different frequency power laws for (a) $\alpha_0 = 10$ dB/cm and (b) $\alpha_0 = 1$ dB/cm measured at 1 MHz.

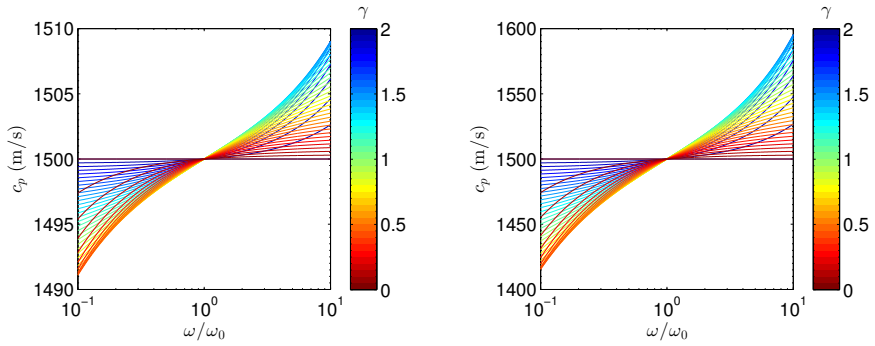


Figure 8.3: Phase velocity obtained for different frequency power laws for (a) $\alpha_0 = 20$ dB/cm and (b) $\alpha_0 = 2$ measured at 1 MHz.

8.2 Nonlinear coherence length

As introduced in Chapter 2, the coherence length magnitude is very helpfully in quantifying the nonlinear acoustic effects in dispersive media. Thus, the efficiency of energy transfer from fundamental to second harmonic component is dependent on the phase matching condition:

$$k\left(2\omega\right) = 2k\left(\omega\right). \tag{8.7}$$

In general, for dispersive media this condition is not fulfilled, so the second harmonic characteristic linear growth develops the well known beating effect (Rudenko et al., 1977), where the beating spatial frequency for the second harmonic is

$$\Delta k_2\left(\omega\right) = \left|2k\left(\omega\right) - k\left(2\omega\right)\right| \tag{8.8}$$

and the coherence length for the second harmonic is defined as

$$x_c\left(\omega\right) = \frac{\pi}{\Delta k_2\left(\omega\right)}. \tag{8.9}$$

In the case study, i.e. in frequency power law attenuation media, using Eqs. (8.5, 8.6), Eq. (8.8) reduces to

$$\Delta k_2\left(\omega\right) = \left(2^\gamma - 2\right)\alpha_0\omega^\gamma \tan\left(\frac{\pi\gamma}{2}\right) \tag{8.10}$$

for $0 < \gamma < 3$ with $\gamma \neq 1$, and

$$\Delta k_2\left(\omega\right)\big|_{\gamma=1} = -\frac{4\log\left(2\right)\alpha_0\omega^\gamma}{\pi} \tag{8.11}$$

for $\gamma = 1$. Then, combining Eq. (8.9) and Eq. (8.10), the characteristic nonlinear coherence length (for second harmonic) can be calculated as

$$x_c\left(\omega\right) = \frac{\pi\cot\left(\frac{\pi\gamma}{2}\right)}{\left(2^\gamma - 2\right)\alpha_0\omega^\gamma} \tag{8.12}$$

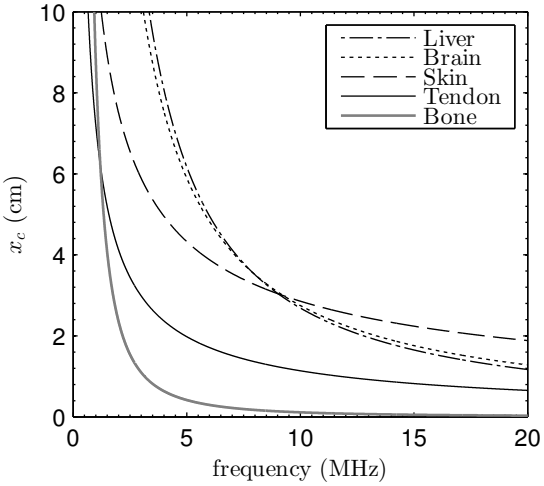


Figure 8.4: Coherence length as a function of frequency for a variety of tissues, where it has been assumed the following power laws: α_{Liver} =0.7 dB/cm/MHz$^{1.2}$, α_{Brain} =0.87 dB/cm/MHz$^{1.1}$, α_{Skin} =3.6 dB/cm/MHz$^{0.6}$, α_{Tendon} =4.77 dB/cm/MHz$^{0.8}$, α_{Bone} =10.5 dB/cm/MHz$^{1.89}$. Typical values extracted from Ref. Hill et al. (2004).

for $0 < \gamma < 3$ and $\gamma \neq 1$, and

$$x_c(\omega)|_{\gamma=1} = \frac{\pi^2}{4\log(2)\,\alpha_0\omega} \tag{8.13}$$

for $\gamma = 1$. It is worth noting here that the coherence length, x_c, is inversely proportional to attenuation magnitude. In this way, in frequency power law attenuation media with strong attenuation values and $\gamma \approx 1$, e.g. in bones, tendons(Fry et al., 1978) where strong dispersion is observed, and also for $\gamma \approx 3$, the efficiency of nonlinear harmonic generation is expected to be modified due to phase mismatching. The frequency dependence for different power laws of real tissues is shown in Fig. 8.4. Here, we show that the magnitude of coherence length is on the order of the size of the internal structures of the human body for ultrasound applications, i.e. $x \lessapprox 10$ cm. Thus, dispersion effects, in addition to attenuation and nonlinear effects can also be important in the nonlinear full solution. However, in order to evaluate the relevance of each effect in the full-wave propagation (attenuation, dispersion and nonlinearity), we shall define the ratio of attenuation to dispersion effects.

Thus, the amplitude of each harmonic will be damped due to the increase in attenuation, following the corresponding power law. Thus, we shall define the second harmonic characteristic attenuation distance for the frequency power law

attenuation media as

$$x_a = \frac{1}{\alpha_0 \omega^\gamma}. \tag{8.14}$$

In this way, using Eq. (8.12, 8.14) we define the quantity N_c as the ratio of attenuation and dispersion effects for power law media as

$$N_c = \frac{x_c}{x_a} = \left| \frac{\pi \cot\left(\frac{\gamma\pi}{2}\right)}{2^\gamma - 2} \right|. \tag{8.15}$$

In the limit of $\gamma \to 1$ Eq. (8.15) reduces to

$$N_c = \frac{\pi^2}{4 \log 2}. \tag{8.16}$$

One important remark is the ratio of attenuation to dispersion effects in a frequency power law media is frequency independent: both, the amount of attenuation and second harmonic phase mismatching magnitude are proportional to the quantity $\alpha_0 \omega^\gamma$. Furthermore, an increase in the attenuation coefficient, α_0, will increase in equal magnitude dispersion and attenuation effects. In this way, as Eq. (8.15) shows, the balance between attenuation and dispersion only depends on the exponent of the frequency power law media.

Figure 8.5 shows the ratio N_c for different power laws. For frequency power laws of $0 < \gamma < 2$, i.e. those that model biological media, the ratio fall in the range $3.43 \lessapprox N_c < \infty$. In this way, $N_c \to \infty$ for dispersionless media, i.e. for even exponent power $\gamma = 0$ and $\gamma = 2$. The higher dispersive regime is obtained for nearly linear frequency dependent absorption, where a local minimum is numerically found at

$$\gamma \approx 1.2053. \tag{8.17}$$

In the range $0.5 < \gamma < 1.5$, the ratio of attenuation to dispersion effects, N_c, present variations of +44% from the minimum value ($N_c = 3.43$).

On the other hand, as Fig. 8.5 shows, for materials with $2 < \gamma < 3$ the dispersive effects can be much more important than attenuation effects. In addition, using Eq. (8.15), we obtain $N_c|_{\gamma=3} = 0$, indicating that dispersive effects strongly

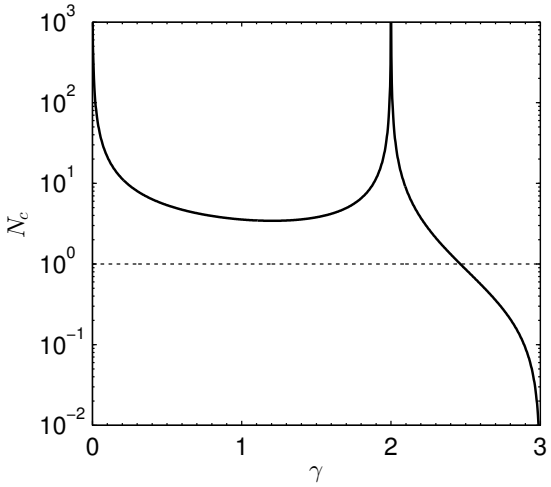


Figure 8.5: Ratio of attenuation versus dispersion, N_c, versus power law exponent γ.

dominates over attenuation effects. However, there exists few materials that falls in this range (Szabo, 1995). For the case of soft tissue media, where $1 < \gamma < 2$, the results arising from this section indicates that attenuation dominates over dispersion effects, but the phase mismatching between forced and propagating second harmonic wave is not negligible for nearly linear frequency dependent attenuation media. However, due to the absorption distance excess in about of one order magnitude the coherence distance, it is not possible to observe a complete beating. Instead, the effect of the weak dispersion in frequency power law media with $1 < \gamma < 2$ is a decreasing in the efficiency of energy transfer from the fundamental to higher harmonics. This aspect will be explored numerically in the next section.

8.3 Competition between nonlinearity and power law attenuation and dispersion

For a monochromatic plane wave in the absence of dissipation, either viscous or relaxation losses, the shock formation distance can be expressed as

$$x_s = \frac{1}{\beta \varepsilon k}, \tag{8.18}$$

with $\varepsilon = v_0/c_0$ as the acoustic Mach number, v_0 the source amplitude, and $\beta = 1 + B/2A$ the parameter of nonlinearity that accounts for material (B/A) and mass advection nonlinearity (unity factor).

In order to measure the relative relevance of nonlinear and attenuation effects, we shall define the so called Gol'dberg number for frequency power law attenuation media as the ratio of characteristic absorption length, x_a, and shock distance, x_s:

$$\Gamma_\gamma = \frac{x_a}{x_s} = \frac{\beta p_0}{c_0^3 \rho_0 \alpha_0 \omega^{(\gamma-1)}}. \tag{8.19}$$

Thus, in the same sense of the classical definition of the Gol'dberg number for thermo-viscous fluids, for $\Gamma_\gamma \gg 1$ the shock distance is too short compared to the characteristic attenuation length and the nonlinear effects dominates over attenuation. In this way, for the range $0 < \gamma < 2$ where the dispersion remains weak, the nonlinear harmonic cascade can be developed and shock waves can be observed. In the limit $\Gamma_\gamma \to \infty$ model equations reduces to lossless nonlinear acoustic and analytical solutions can be obtained for a variety of boundary conditions (e.g. in the case of monochromatic plane wave propagation the well known Fubini-Blackstock-Fay solution describes the harmonic evolution). On the other hand, in the regime $\Gamma_\gamma \ll 1$ dissipation effects dominates over nonlinear effects. Although energy transfer from fundamental to higher harmonics could be observed, absorption prevents the development of shock waves. In the limit of $\Gamma_\gamma \to 0$, linear-damped propagation is achieved and no harmonic is generated.

However, in many practical cases $\Gamma_\gamma \approx 1$ and an analytical treatment of the problem is not available (with the exception of $\gamma = 2$ where the so called Mendousse, Eq. 7.32, solution could be obtained). Due to plane-harmonic nonlinear wave propagation in a mono-relaxing media is still unsolved, the prospective is fair in order to find an exact analytical solution for multiple relaxation media or for a continuum of relaxation processes. In addition, no analytical solution is available for fractional derivatives nonlinear wave equations (Szabo, 1994) for the case of monochromatic plane wave. Thus, in this section we will explore numerical solutions of Eqs. (7.1, 7.2, 7.10, 7.8) by using the methods described in Chapter 7 in order to study the harmonic generation in frequency power law attenuation media.

In addition, one important remark arising from Eq. (8.19) for tissues with exact $\gamma = 1$ is that the ratio between nonlinearities and attenuation effects does not depend on frequency. In this way, Eq. (8.19) predicts that given media parameters, (β, c_0, ρ_0 and α_0), a wave with fixed initial amplitude will develop exact nonlinear processes with independence of the wave frequency. In this way, the amplitude can be selected and fixed in order to produce shock waves as

$$p_0 > c_0^3 \rho_0 \alpha_0 / \beta. \tag{8.20}$$

If the frequency is increased the shock formation distance is moved towards the source, but according to Eq. (8.19) the Gol'dberg ratio remains constant and therefore the harmonic balance remains the same but stretched in space.

As explained above, for $\Gamma_\gamma \approx 1$ the nonlinear and attenuation effects may play a role of similar importance in the full solution. Thus, there exist a competition between nonlinearity and attenuation effects that, at first order, leads the final amplitude for each harmonic. In one hand, harmonic generation is governed by nonlinearity, where second and higher harmonics are generated by cascade processes due to material nonlinearity and mass convection processes. On the other hand, each generated harmonic will be attenuated during propagation by its specific attenuation coefficient, provided by the frequency power law evaluated at each harmonic frequency.

Consider here media with equal attenuation at fundamental frequency, but different power law. In these media, it is obvious that for higher values of the power law exponent, γ, the attenuation of higher harmonics will be in any case higher than the attenuation for media with lower power law. Thus, in principle, the exponent has a great influence in the harmonic balance of the traveling nonlinear wave due to differences in attenuation, and these differences will be higher for higher harmonics.

However, as long frequency power law attenuation introduces dispersion, see Eq. (8.2), the phase matching conditions are in general no longer fulfilled. Therefore, dispersion modifies the efficiency on harmonic generation, together with the interplay between power law attenuation and nonlinear harmonic growing. Thus, from Eqs. (8.10, 8.11), phase matching conditions, i.e. $\Delta k_2 = 0$, are fulfilled for even powers, e.g. $\gamma = 0, 2, \ldots$. In these cases, propagation is nondispersive: the nonlinear efficiency is maximum and therefore the energy transference from fundamental to higher harmonics is maximized. On the other hand, for $\gamma \approx 1$, dispersive propagation is predicted and the nonlinear efficiency will be modified. Due to these effects cannot be isolated, we study the modification of the nonlinear efficiency numerically.

8.4 Plane wave simulations in power law media

As shown Chapter 7, the propagation of nonlinear acoustic waves in frequency power law attenuation can be modeled by the use of multiple relaxation processes. Thus, the set of Eq. (7.1, 7.2, 7.10 and 7.8) can be expressed for a plane wave travelling in x direction as

$$\frac{\partial \rho}{\partial t} = -\frac{\partial (\rho v_x)}{\partial x}, \tag{8.21}$$

$$\frac{\partial v_x}{\partial t} = -\frac{1}{\rho}\frac{\partial p}{\partial x} - \frac{1}{2}\frac{\partial v_x^2}{\partial x} + \frac{1}{\rho}\left(\frac{4}{3}\eta + \zeta\right)\frac{\partial^2 v_x}{\partial x^2}, \tag{8.22}$$

$$p = c_\infty^2 \rho' + \frac{c_0^2}{\rho_0}\frac{B}{2A}\rho'^2 - \sum_{n=1}^{N} S_n, \tag{8.23}$$

$$\frac{\partial S_n}{\partial t} = -\frac{1}{\tau_n} S_n + \frac{\eta_n c_0^2}{\tau_n}\rho', \tag{8.24}$$

where v_x is the x component of particle velocity vector.

In order to study the changes induced by power law attenuation and dispersion into the nonlinear efficiency, we consider media with equal attenuation coefficient at fundamental frequency, ω_0, as shown in Fig. 8.2. Thus, by varying power law exponent from realistic values for biological media, $\gamma = [0.5, 2]$, dispersion is introduced while the attenuation of the fundamental wave remains constant. As Eq. (8.15) shows, the balance between attenuation and dispersion for power law media (N_c) only depends on the power law exponent. In this way, by increasing the attenuation magnitude both dispersion and attenuation effects will by modified in same amplitude. On the other hand, by modifying the attenuation magnitude the Gol'dberg number for power law media is also modified following Eq. (8.19). In summary, for media with equal attenuation coefficient at fundamental frequency, the balance between nonlinearity and attenuation effects, Γ_γ is governed by the attenuation coefficient, while the balance between attenuation and dispersion effects, N_c, is governed by the exponent of the power law.

Numerical results for the spatial distribution of fundamental wave are shown in Fig. 8.6, while the spatial distribution for second and third are plotted in Fig. 8.7. The amplitude and fundamental wave of the excitation was maintained constant, thus, by changing attenuation magnitude the ratio between attenuation and nonlinearity is modified and therefore the ratio between dispersion and nonlinearity also is modified.

Here, the analytical nonlinear solution for lossless media (Bessel-Fubini's solution) is plotted in dotted line. Thus, for low attenuation media, i.e. when $\Gamma_\gamma \to \infty$, nonlinear effects dominate over attenuation and dispersion and therefore the numerical solution for frequency power law media converges to the lossless Bessel-Fubini's solution, see Fig. 8.6 and Fig. 8.7 for $\Gamma_\gamma = 57.9$. In these cases, the fundamental wave decay is mainly due to energy transference to higher harmonics, that grow with propagation. Here, harmonic amplitude is independent on the exponent of the power law, showing that both dispersion and attenuation effects are much less smaller compared with nonlinear effects during propagation and can be neglected for $\Gamma_\gamma \to \infty$.

In contrast, as Figs. 8.6, 8.7 show for $\Gamma_\gamma = 0.74$, for high damped media and weak nonlinearity, attenuation effects are comparable to nonlinear harmonic pumping. The fundamental wave not only decays for energy transfer but also due to high attenuation.

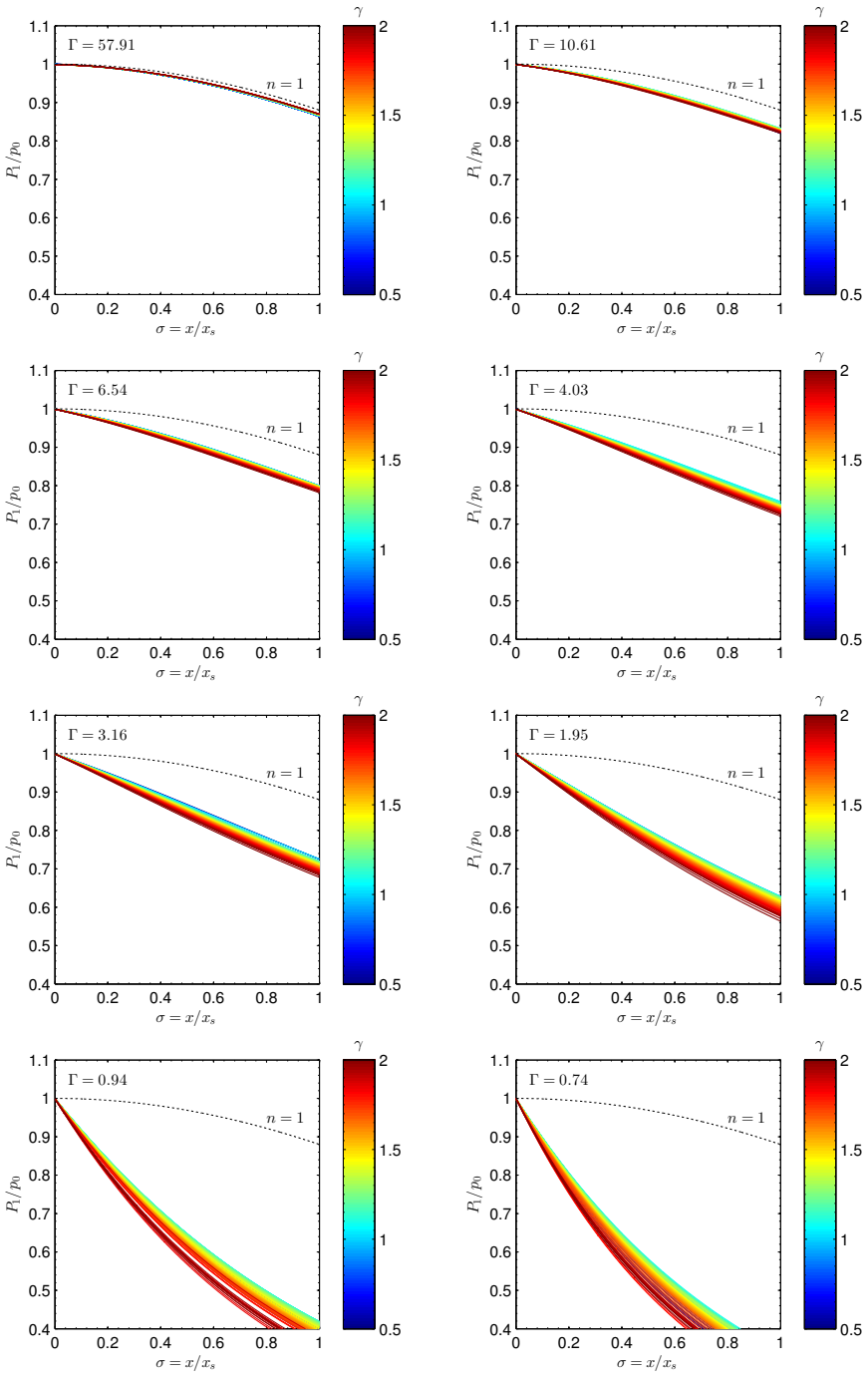


Figure 8.6: First harmonic normalized-amplitude spatial distribution for different frequency power laws. For each subplot, the ratio of nonlinear to power law attenuation effects, Γ_γ, is increased

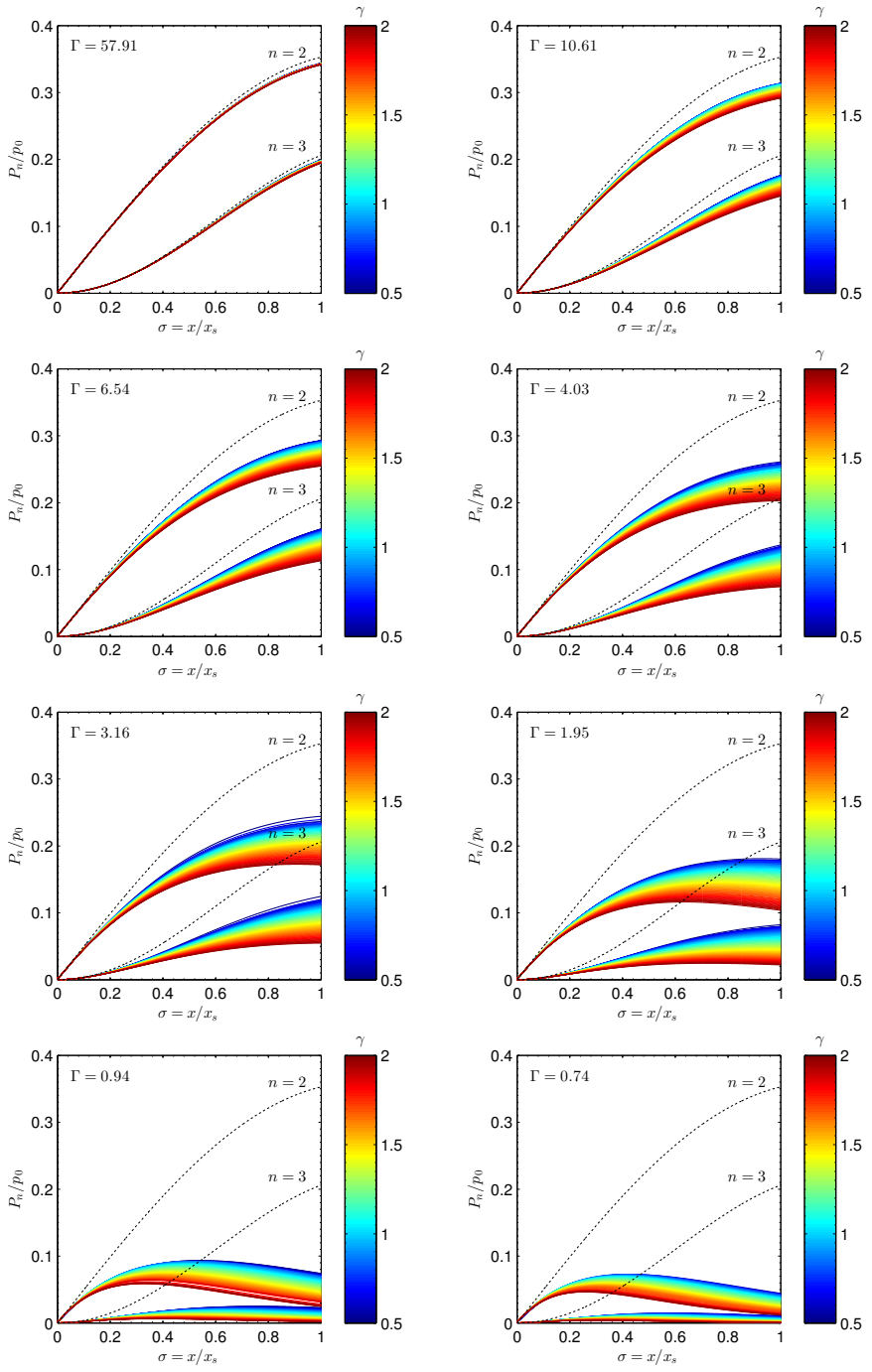


Figure 8.7: Second and third harmonic normalized-amplitude distribution for different frequency power laws. For each subplot, the ratio of nonlinear to power law attenuation effects, Γ_γ, is increased

Thus, at distance $\sigma \approx 0.5$ fundamental wave have loss approximately half of its initial amplitude and therefore nonlinear energy transfer processes to second-and-higher harmonics also diminishes. On the other hand, second and third harmonics are mainly generated near the source, where fundamental wave is still have enough amplitude. However, attenuation of higher harmonics is in any case higher than for fundamental wave and therefore they are quickly damped by the power law lossy media. Due to the harmonic generation is strongly decreased far away from the source due to fundamental wave energy loss, second and higher harmonics are restricted near the source and its maxima value is produced for $\sigma < 1$, in contrast with lossless media where the maxima of the harmonics is produced $\sigma \approx \pi/2$.

It is worth noting here that the harmonic evolution is strongly dependent on the exponent of the power law. Thus, due to differences in attenuation coefficient for each harmonic (see Fig 8.2 for $\omega/\omega_0 = 2$), second-and-higher harmonic amplitude is damped by different magnitude, where obviously higher attenuation and therefore lower harmonic amplitude is observed for the cases of $\gamma \to 2$.

However, although the fundamental wave attenuation magnitude is the same, with independence of the power law exponent, the amplitude of the fundamental wave strongly varies. We recall here to Eq. (8.15), that shows the ratio between dispersion and attenuation. By varying the power law exponent dispersion is modified. Thus, the harmonic efficiency is only maximized for even powers of γ, where for $\gamma \approx 1$ dispersion effects are not negligible. This is the reason because more energy remains in the fundamental wave for $\gamma \approx 1$, dispersion is modifying the phase matching conditions and therefore the energy transfer from fundamental to second-and-higher harmonics is decreased.

8.5 Nonlinear efficiency

As explained above, the nonlinear efficiency can be strongly dependent not only on the magnitude of the attenuation, but also on the dispersion due to frequency power law attenuation. These effects have been shown previously for tissue like media in the absence of dispersion (Haran et al., 1983) and including power law dispersion (Kashcheeva et al., 2000; Wallace et al., 2001) for selected media. A closer view of these phenomena can be studied by showing the harmonic amplitude at a given distance, that for reference we choose $\sigma = 1$. Thus, Fig. 8.8 shows the amplitude of the fundamental wave for different power law media and its dependence on the power law. As commented above, if the balance between nonlinear and attenuation effects is constant, the maximum amplitude of the fundamental component is observed for power laws where dispersion is maximized, i.e. for $\gamma \approx 1.2$. Furthermore, there exist differences between different Gol'dberg numbers: the balance between nonlinearity and dispersion is also coupled to the attenuation, so for high Gol'dberg numbers dispersion effects also dominate over nonlinear effects, leading to a decreasing in the nonlinear efficiency and therefore

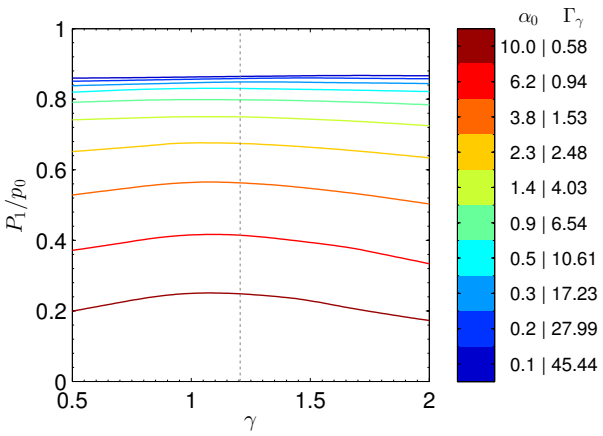


Figure 8.8: Amplitude of the fist harmonic for different Gol'dberg number (Γ_γ) in function of the exponent of the frequency power law (γ), measured at shock formation distance, $\sigma = 1$. The attenuation of the media is selected for achieve a constant value at first harmonic frequency, so for this plot the amount of media attenuation is independent of the power law.

more energy remains in the fundamental component of the nonlinear wave.

A knowledge of the role of the power law dispersion into the second-and-higher harmonic components is not so evident. If dispersion is modified, i.e. we force a change in the power law exponent, the attenuation magnitude at second harmonic frequency will be also modified. On the other hand, is obvious that if attenuation is matched for second harmonic, e.g. being the source frequency $\omega_0/2$ in Fig. 8.2, the attenuation magnitude at fundamental wave will be different.

Left side of Fig 8.9 shows the harmonic amplitude in function of the power law exponent at distance $\sigma = 1$ for different Gol'dberg ratios. Observing the harmonic amplitude is not obvious that, as stated, more energy is transferred for nondispersive power law media ($\gamma \to 0, 2, ...$). Thus, as attenuation is strongly increased for second harmonic in function of the power law exponent, the harmonic amplitude is therefore more attenuated for the non-dispersive cases, masking the effect of nonlinear efficiency.

In this way, we introduce in the right side of Fig 8.9 a compensation of the second harmonic amplitude by the attenuation coefficient at this frequency. In this plot, it is appreciable that for nondispersive cases, $\gamma = 2$, the harmonic amplitude is higher due to the phase matched generation, while for the dispersive cases there exist a reduction in the efficiency for second harmonic generation. However, this compensation does not take into account that harmonics are generated *during* propagation. Thus, it serves as an eye guide for illustration purposes but lacks of exact physical fidelity.

Similar plots, shown in Fig. 8.10, are generated for third harmonic at shock

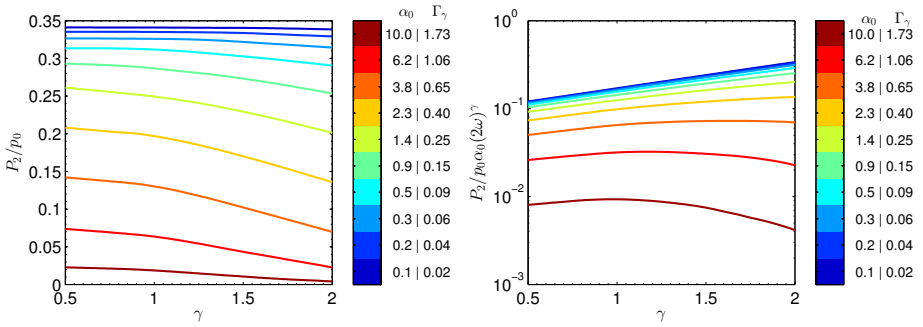


Figure 8.9: Left: Amplitude of the second harmonic for different Gol'dberg number (Γ_γ) in function of the exponent of the frequency power law (γ), measured at shock formation distance, $\sigma = 1$. Right: Same curves compensated by the increment of attenuation of second harmonic, which is different for each power law.

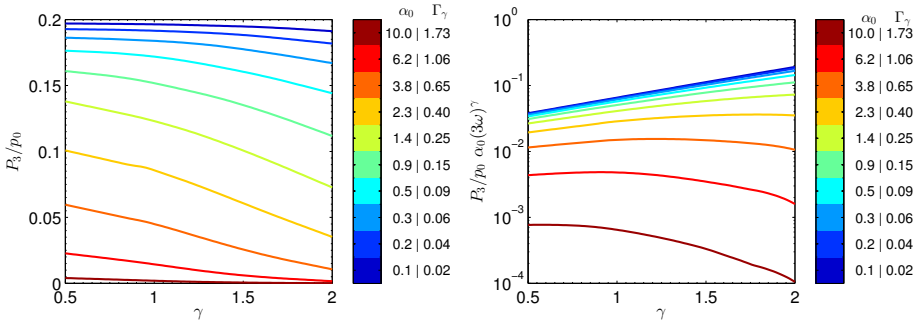


Figure 8.10: Left: Amplitude of the third harmonic for different Gol'dberg number (Γ_γ) in function of the exponent of the frequency power law (γ), measured at shock formation distance, $\sigma = 1$. Right: Same curves compensated by the increment of attenuation of third harmonic, which is different for each power law.

formation distance. Here, the amplitude is lower compared to second harmonic due to nonlinear generation. In this case, for a given Gol'dberg ratio the differences in the harmonic amplitude between different power laws increases, mainly due to the increasing in the attenuation coefficient at third harmonic frequency. Moreover, if the attenuation of each harmonic amplitude is compensated, as shown in right hand side of Fig. 8.10, the behavior is the similar than the observed to the second harmonic efficiency.

8.6 Phase changes induced by dispersion

From the dispersion relations for power law media, showed in Fig.8.1, it is appreciable that second harmonic component propagates, for $0 < \gamma < 2$, faster than

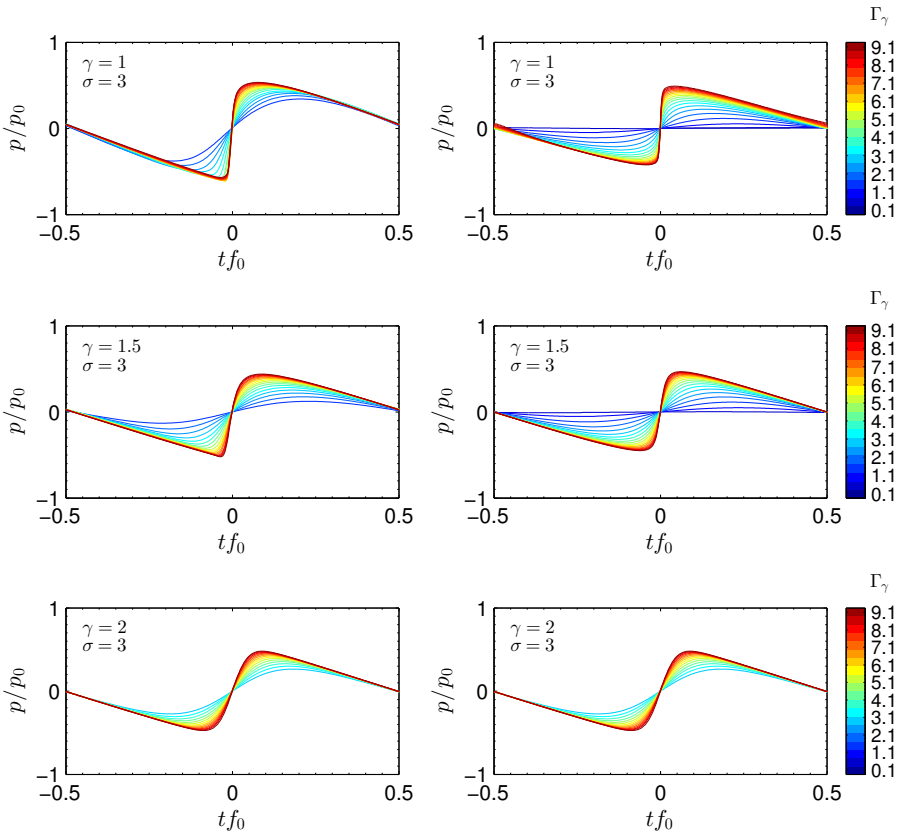


Figure 8.11: Waveforms calculated for (left) dispersive power law media at distance $\sigma = 3$ and (right) artificial dispersionless only taken into account power law absorption. From up to down the power law exponents ranges are $\gamma = [1, 1.5, 2]$

fundamental wave. The second harmonic that is generated near the source, after propagation, will sum with the harmonics at higher distances. Due to the locally generated second harmonic waves are in phase with fundamental wave, there exist a phase difference between the forced (locally generated) and the background propagation second harmonic wave. This phase shift can be predicted from dispersion relations, as is dependent to phase matching conditions (Eq.8.8). In the case of second harmonic, a complete phase shift between propagating and forced waves occurs every $x = 2x_c$. In this way, as explained in Section 8.5, these processes modify the efficiency of the nonlinear generation in frequency power law attenuation media.

In addition, these phase changes also modify the shape of the nonlinear waveforms in frequency power law media. The shape of a nonlinear waveform is determined by its specific harmonic balance, but also the relative phase between

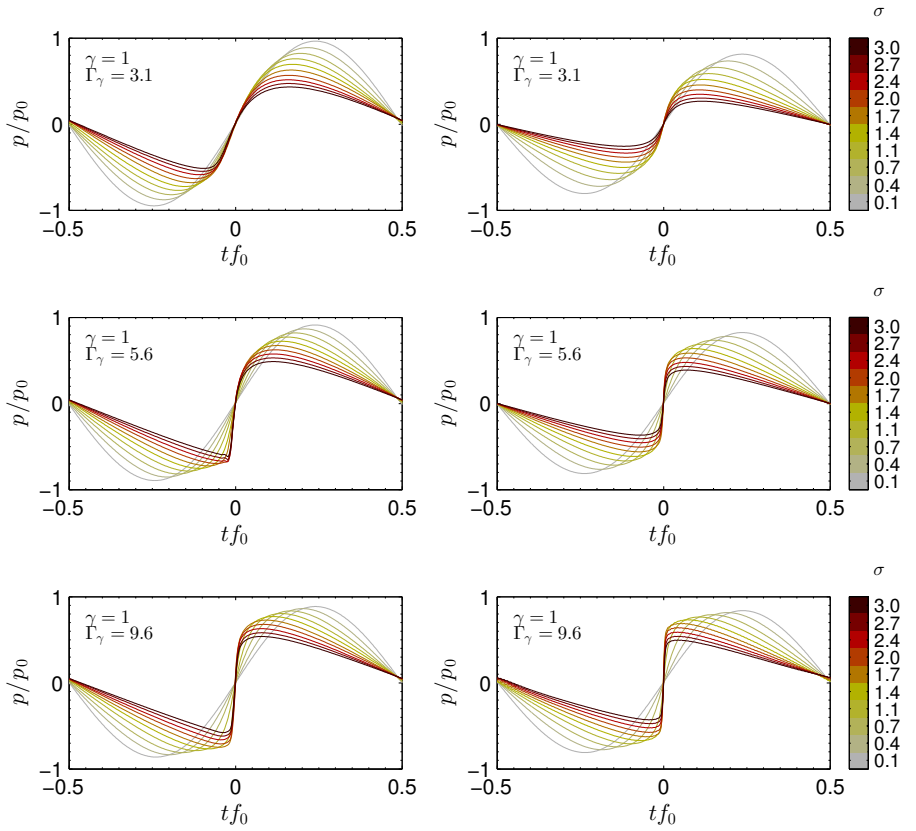


Figure 8.12: Waveform evolution calculated for linear power law ($\gamma = 1$). (Left) dispersive propagation. (Right) nondispersive simulation for comparison using artificial dispersionless power law absorption. From up to bottom the ratio between nonlinear and attenuation (Γ_γ) effects is increased.

spectral components. In nondispersive media, the harmonic balance is a competition between nonlinearity and absorption processes. As seen in this Chapter, dispersion of power law media modifies this balance. Moreover, the relative phase between spectral components will be also modified due to dispersion and it will change the shape of the waveform.

To study these effects, we use a k-space pseudospectral method (Treeby et al., 2010; Treeby et al., 2012) to evaluate one dimensional nonlinear propagation. This method, through the spectral representation of the field, provides an efficient way to evaluate the linear integro-differential operator based fractional Laplacian that introduces frequency power law attenuation. This also provides a way to eliminate dispersion and evaluate only a nondispersive version of the frequency power law operator.

Thus, Fig. 8.11 shows the nonlinear waveforms measured at distance $\sigma = 3$ including dispersion and an artificial nondispersive version of the frequency power law attenuation operator in the k-space. As can be seen, the specific shape of the waveform depends on the exponent of power law: it provides a balance in the harmonic magnitude through attenuation processes and the above described changes on the efficiency through dispersion processes.

However, if the power law attenuation is maintained but dispersion is artificially not included in the calculations, there can be seen that the waveforms shape presents several changes. Thus, as Fig. 8.11 shows, dispersion breaks the symmetry of the nonlinear waveforms. In the case of nondispersive propagation the waveforms for $\Gamma_\gamma \gg 1$ converge to the well-known sawtooth waves as predicted by the Fubini-Blackstock-Fay solution (Hamilton et al., 1998a). For intermediate Γ_γ values, due to different balance in harmonic attenuation during propagation, the shape of the final waveforms is also slightly changed. However, in this case of artificially nondispersive propagation, the shape of the waveforms conserve the symmetry between compression and rarefaction cycles typical of sawtooth waves.

In contrast, this symmetry is broken for the waveforms generated including dispersion, in the same sense as in other dispersive systems as mono-relaxing fluids (Hamilton et al., 1998a). A more detailed frame for $\gamma = 1$ is presented in Fig. 8.12, where the complete evolution of the waveforms is represented in each frame. Here it can be seen how the shock front is smoothed in the compression phase, while remains sharp in the negative rarefaction phase.

8.7 Conclusions

In this chapter we have revised the fundamental problem of the competition between nonlinear and attenuation effects in frequency power law attenuation media, with special emphasis in the effects of the weak dispersion. We have derived simple expressions in order to quantify the role of the exponent of the power law in the balance between nonlinearity, dispersion and attenuation. The results show that the dispersion effects present more relevance in the nonlinear propagation for media obeying $\gamma \approx 1.2$, where the ratio between nonlinear characteristic distance and weak dispersion characteristic distance present its minimum. Detailed numerical examples are given in agreement with this predictions. This situation is of special interest due to most soft tissues typically present values of the power law exponents around this critical value.

The efficiency in the harmonic generation is studied numerically, showing that power law dispersion modifies the cumulative energy transfer to higher harmonics. Thus, considering a media with same attenuation value at the fundamental component, more energy remains in the fundamental harmonic component in the cases of nearly linear power law. On the other hand, in frequency power law

media attenuation effects are of higher importance in the nonlinear propagation than weak dispersion effects. However, we have shown that the waveform shape also strongly depends on the weak dispersion, where the characteristic asymmetric profile is observed for dispersive frequency power law attenuation.

In real situations, where other phenomena must to be included (beam diffraction, tissue scattering and inhomogeneities, ...), it becomes far more complicated to study the role of each effect in the nonlinear propagation. Thus, plane wave propagation offers the possibility to isolate some of the physical mechanisms that governs nonlinear propagation (in this case attenuation and dispersion) and to understand the balance between them. The results presented in this chapter, far from present completely new physics, offers detailed calculations and a broad view of this fundamental problem.

References

Fry, FJ and JE Barger (1978). "Acoustical properties of the human skull". In: *The Journal of the Acoustical Society of America* 63.5, pp. 1576–1590.

Hamilton, Mark F, David T Blackstock, et al. (1998a). *Nonlinear acoustics*. Vol. 237. Academic press San Diego.

Haran, Michael E and Bill D Cook (1983). "Distortion of finite amplitude ultrasound in lossy media". In: *The Journal of the Acoustical Society of America* 73.3, pp. 774–779.

Hill, C.R., J. C. Bamber, and G.R. ter Haar (2004). *Physical Principles of Medical Ultrasonics, 2nd ed.* John Wiley & Sons Ltd, Chichester, England.

Kashcheeva, S.S., O.A. Sapozhnikov, V.A. Khokhlova, M.A. Averkiou, and L.A. Crum (2000). "Nonlinear distortion and attenuation of intense acoustic waves in lossy media obeying a frequency power law". In: *Acoustical Physics* 46, pp. 170–177.

O'Donnell, M., E. T. Jaynes, and J. G. Miller (1981). "Kramers–Kronig relationship between ultrasonic attenuation and phase velocity". In: *J. Acoust. Soc. Am.* 69.3, pp. 696–701.

Rudenko, O.V. and S.I. Soluian (1977). *Theoretical foundations of nonlinear acoustics*. Studies in Soviet science. New York, NY 10011, USA: Consultants Bureau, p. 274.

Szabo, Thomas L (1994). "Time domain wave equations for lossy media obeying a frequency power law". In: *J. Acoust. Soc. Am.* 96.1, pp. 491–500.

Szabo, Thomas L (1995). "Causal theories and data for acoustic attenuation obeying a frequency power law". In: *J. Acoust. Soc. Am.* 97.1, pp. 14–24.

Treeby, Bradley E and BT Cox (2010). "Modeling power law absorption and dispersion for acoustic propagation using the fractional Laplacian". In: *J. Acoust. Soc. Am.* 127.5, pp. 2741–2748.

Treeby, Bradley E, Jiri Jaros, Alistair P Rendell, and BT Cox (2012). "Modeling nonlinear ultrasound propagation in heterogeneous media with power law absorption using a k-space pseudospectral method". In: *J. Acoust. Soc. Am.* 131.6, pp. 4324–4336.

Wallace, Kirk D, Mark R Holland, and James G Miller (2001). "Improved description of shock wave evolution in media with frequency power law dependent attenuation". In: *The Journal of the Acoustical Society of America* 109.5, pp. 2263–2265.

Waters, Kendall R, Michael S Hughes, Joel Mobley, Gary H Brandenburge, and James G Miller (2000). "On the applicability of Kramers–Krönig relations for ultrasonic attenuation obeying a frequency power law". In: *The Journal of the Acoustical Society of America* 108.2, pp. 556–563.

Waters, Kendall R, Joel Mobley, and James G Miller (2005). "Causality-imposed (Kramers-Kronig) relationships between attenuation and dispersion". In: *Ultrasonics, Ferroelectrics and Frequency Control, IEEE Transactions on* 52.5, pp. 822–823.

Publications

The contents of this chapter have been presented in the following publications:

Conference proceedings

- **Jiménez, N.**; Redondo, J.; Sánchez-Morcillo, V.; Iglesias, P. C. and Camarena, F. "On the Nonlinear Effects in Focused Ultrasound Beams with Frequency Power Law Attenuation" *43rd Annual UIA Symposium*, Madrid, Spain. 23 - 25 April. In: *Physics Procedia*, Volume 63, 2015, Pages 47-53, (2014)